sciendo

Transport and Telecommunication, 2019, volume 20, no. 3, 191–204
Transport and Telecommunication Institute, Lomonosova 1, Riga, LV-1019, Latvia
DOI 10.2478/ttj-2019-0016

IDENTIFYING VEHICLE AND COLLISION IMPACT BY APPLYING THE PRINCIPLE OF CONSERVATION OF MECHANICAL ENERGY

Stanimir Karapetkov [1], Lubomir Dimitrov [2], Hristo Uzunov [3] and Silvia Dechkova [4]

[1,3,4] Technical University of Sofia, Faculty and College – Sliven, Bulgaria
[1] skarapetkov@yahoo.com
[2] Technical University of Sofia, Bulgaria
lubomir_dimitrov@tu-sofia.bg
[3] hvuzunov@gmail.com
[4] sdechkova@tu-sofia.bg

Various methodologies and tools applied to identification of vehicle and collision impact seek to present more and more accurate solutions to reproduce, restore, recreate and investigate the casualty. Modern computer technology and software provide the tools to solve specific problems developing mathematical modelling of complex mechanical systems involving vehicles and other objects in a road accident. Scientists generally utilize the Standard Test Method for Impact Testing calculating the energy of deformation of both vehicles, however, one of its limitations is the evaluation of the kinetic energy of the vehicles in post-collision taking into consideration vehicle rotation and linear displacement. To improve the analysis, dynamic traffic simulation is used, taking into account the variations in the coefficient of friction, suspension elasticity and damping. The proposed method is based on a system of two equations derived from two principles: the Principle of Conservation of Mechanical Energy and the Principle of Conservation of Momentum in the impact phase. The new approach is conducted on mathematical modelling and computer simulation of vehicle motion after the impact, wherefrom the linear and angular velocities are analysed. This is achieved by the numerical solution of the differential equations of motion of the cars after the impact, and the given initial conditions that satisfy the solution are used to solve the system of equations. The main findings of the study can be grouped as follows: 1) The positions of the vehicles prior to the moment of first impact and the post-impact orientation of velocity vectors are more precise. 2) The variability of the tire-road friction coefficient is taken into consideration. 3) The value of coefficient of restitution according to Newton's theory of impact is unnecessarily determined.

Keywords*:* identification, impact, vehicles, MATLAB

1. Introduction

Dynamic crash tests are main tasks for expert assessment of road traffic accidents. As a result, the velocity of the centres of mass of the two vehicles is obtained (Schmidt *et al*., 1998; Sharma *et al*., 2007; Daily *et al*., 2006; Prasad, 1990; Stucki, 1998; Hight *et al*., 1985; Mchenry R. and Mchenry G., 1986; Wach, 2003). There are different methods of dynamic analysis, each with certain inaccuracy of the results obtained. The greatest error rate occurs when trying to find the impact, because the velocity of movement of the centres of mass after the impact is determined by the Centre-of-Mass Motion Theorem. Vehicles are considered to be material points and the tire-road friction coefficients are estimated. The effect of post-impact vehicle rotation and the resulting angular velocity are not taken into account. It is a well-known fact that after the crash the vehicle is involved in a significant rotation, each tire continues moving with a relative lateral sliding motion, which is a combination of linear displacement and simultaneous rotation. Due to significant deformations, it is also possible that a wheel might be blocked which would produce a much greater frictional force component compared to the frictional force of the wheel rotation with simultaneous lateral sliding. This movement is subjected to complex dynamic research owing to the fact that the tire-road friction coefficient is practically variable and depends on the speed of the point of contact.

2. Dynamic Impact Analysis between Two Vehicles

The most commonly used method of car impact is based on the Law of Momentum Conservation (Nolan *et al*., 1998; Hibbeler, 2004; Karapetkov, 2005; Karapetkov, 2010), which can be expressed as:

$$\vec{Q} = m_1\vec{V}_1 + m_2\vec{V}_2 = m_1\vec{u}_1 + m_2\vec{u}_2, \quad (1)$$

where:

m_1 and m_2 – masses of vehicles,

$\vec{V}_1$ and $\vec{V}_2$ – pre-impact velocities of the centres of mass of the two vehicles,

$\vec{u}_1$ and $\vec{u}_2$ – post-impact velocities of the centres of mass of the two vehicles.

The vector equation is projected on two mutually perpendicular axes, yielding a system of two equations with two unknowns.

Based on the centre-of-mass motion theorem the two cars after collision get:

$$m_k \frac{d\vec{u}_k}{dt} = \sum \vec{F}_i, \quad (2)$$

where:

$m_k/k = 1,2/$ – total mass of each automobile,

u_k – post-impact vehicle velocity of the centre of mass,

$\vec{F}_i$, $/i = 1,2,\ldots n/$ – resistance forces and weight. Resistance forces are velocity-oriented of each contact tire-road point and opposite in direction. After projecting the centre of mass trajectory upon the tangential vector $\vec{\tau}$ and changing the variable, it is obtained:

$$m_k \frac{du_k}{ds_k} = \sum F_{i\tau}, \quad (3)$$

where:

s_k – curvilinear abscissa for the trajectory of the vehicle centre of mass.

Dividing the variables and integrating for the post-impact rest position time interval the following occurs:

$$\int_0^1 u_k du = \int_0^1 \sum F_{i\tau}\, ds\,. \quad (4)$$

Using integration we can obtain:

$$u = \sqrt{2\sum_{i=1}^{n} j_i\sigma_i}, \quad (5)$$

where:

σ_i, $/i = 1,2,\ldots n/$ – is the distance that the centre of mass has moved the vehicle.

If the road has a tilting slope "+" or a downhill "-" and the weight action of the vehicle is taken into account, the acceleration of the post-impact vehicle centre of mass is:

$$j_i = [\mu_i cos\alpha_i \pm sin\alpha_i]g, \quad (6)$$

where:

μ_i, $/i = 1,2,\ldots n/$ – friction coefficient for the particular road section of the real-time motion trajectory of the post-impact vehicle centre of mass (James *et al*., 1994),

α_i $/i = 1,2,\ldots n/$ – the road inclination angle for the particular road section of the trajectory of the real-time motion trajectory of the post-impact vehicle centre of mass,

g – acceleration of gravity.

The current study has probably some limitations due to the fact that vehicles are regarded as material points, on the one hand and on the other, the dynamic analysis does not take into account the variability of the road-tire friction coefficient, elasticity of suspension, post-impact angular velocity of the two vehicles.

3. Identification of Impact between Passenger Cars

Determining the velocity of the vehicle centre of mass following typical errors depends mainly on the correct definition of initial data. It is obvious that errors in the established methods of investigation are

mainly made by selecting the tire-road friction coefficient. In practice, the motion is planar, but apart from linear displacement there is a complex dynamics of rotation of a multi-mass system of bodies.

Consequently, a new approach to vehicle dynamics has been implemented taking into consideration not only the post-impact linear displacement of the two passenger cars but also their rotation and deformation energy (Wicher, 2006). Integrating equation (1) to the Principle of Conservation of Mechanical Energy, it results in:

$$\frac{m_1 V_1^2}{2} + \frac{m_2 V_2^2}{2} = \frac{m_1 u_1^2}{2} + \frac{m_2 u_2^2}{2} + \frac{I_1 \omega_1^2}{2} + \frac{I_2 \omega_2^2}{2} + E_1 + E_2, \quad (7)$$

where:

m_1 and m_2 – masses of vehicles
I_1 and I_2 – mass inertia for the two vehicles around the vertical axis Oz,
V_1 and V_2 – pre-impact vehicle velocities of the centre of mass,
u_1 and u_2 – post-impact vehicle velocities of the centre of mass,
ω_1 and ω_2 – post-impact angular velocities of the vehicle bodies around the vertical axis Oz,
E_1 and E_2 – deformation energy of car bodies resulting in a crash.

According to the Law of Momentum Conservation in a two-vehicle impact the analysis includes post-impact velocity of the vehicle centre of mass. When designing the equation on two mutually perpendicular axes in the right-hand side of the equation system, the post-impact velocity of the centre of mass is present. Typical error of the method is to determine the exact direction of the vehicle motion after the impact. The velocity vector is adopted in the direction of the coordinates of the centres of mass at the moment of impact and the final rest position. In practice, the car performs a sophisticated spatial movement that includes rotation and translation, as well as complex dynamics of tire-road friction.

The new approach in the study aims to analyses the post-impact velocity motion of the centre of mass, taking into account the macro motion of the multi-mass system, as well as the elasticity of suspension, the damping and the variable nature of the friction coefficient. Improved accuracy of the analysis is achieved by the fact that the vehicle is not considered a physical point that changes its direction of motion as a result of the impact and the created impulse by the impact force. In addition to the linear motion, the rotation around the vertical axis is also taken into account.

The analysis can be used primarily in car-to-car collisions. Car crash study of passenger cars and heavy goods vehicles, when there is a significant difference in masses, is not a matter of the present review.

4. Estimation of Deformation Energy of Vehicle

(Campbell, 1974; Owsiański, 2007)

According to that model the intensity of the distributed impact load / dimension [N / m] / is considered a linear function of the plastic deformation.

Hence, to determine deformation energy, it is assumed that the intensity of the distributed load of the impact forces is a linear function of the plastic deformation and is determined by the formula

$$\frac{dF}{dl} = q = A + Bc, \quad (8)$$

where:

F is the impact force; c – value of the plastic deformation, measurement performed perpendicularly to the respective contact plane under impact/deformation depth); l – axis, perpendicular to the measured contact deformation and lying in the plane, where plastic deformation results. The maximum value of the coordinate l is the width of deformation zone L. Here, the coefficient A characterizes the elasticity of the structure and has a dimension of [N / m], whereas B – characterizes the linear increase with a dimension of $[N/m^2]$.

Figure 1 shows the change in the intensity of the distributed load of the impact forces as a linear function of the plastic deformation. The maximum elastic deformation, which magnitude is $\delta = A/B$ – i.e. the length of the leg of the rectangular triangle, whose area is denoted by G. The elastic force has an intensity of the distributed load that can be assumed to be linear

$$q_e = \frac{dF}{dl} = Bc, \quad (9)$$

where: c - total elastic strain whose maximum value is $\delta = A/B$.

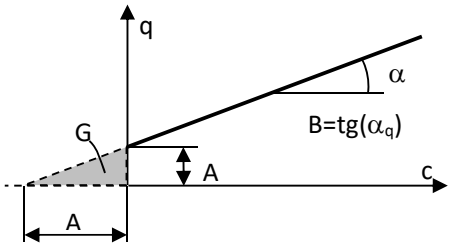

Figure 1. Impact intensity and plastic deformation dependence

The relative energy of elastic and plastic deformation per unit width is determined by the integral

$$dE = \left[\int_0^{\delta} q_e dc + \int_0^{c} q dc\right] dl$$

$$dE = \left[\int_0^{\delta} Bc dc + \int_0^{c} (A + Bc) dc\right] dl \tag{10}$$

$$dE = \left[G + Ac + B\frac{c^2}{2}\right] dl,$$

where it is laid

$$G = \frac{B}{2}\delta^2 = \frac{A^2}{2B}. \tag{11}$$

The value of G represents the area of the indicated triangle in Figure 1 and, if integrated in the plastic deformation, is an integration constant.

The total energy loss is determined for the entire deformation width L by the integral

$$E = \int_0^L dE = \int_0^L \left[\frac{A^2}{2B} + Ac + B\frac{c^2}{2}\right] dl,$$

$$E = \int_0^L \left[Ac + B\frac{c^2}{2}\right] dl + \frac{A^2}{2B} L. \tag{12}$$

Deformation is a function of the transverse projection of *l*. After solving the integral for 6 uniformly distributed points along the deformation width, the following formula is obtained

$$E = (1 + tg^2\theta_s)\frac{L}{5}\left[\frac{A}{2}(c_1 + 2c_2 + 2c_3 + 2c_4 + 2c_5 + c_6) + \frac{B}{6}\left(c_1^2 + 2c_2^2 + 2c_3^2 + 2c_4^2 + 2c_5^2 + c_6^2 + c_1c_2 + c_2c_3 + c_3c_4 + c_4c_5 + c_5c_6\right) + 5\frac{A^2}{2B}\right], \tag{13}$$

where:

θ_s – angle between impact normal and impact impulse;

L – width of deformation depth in $[m]$;

c_i /i = 1,2 ... 6/ – magnitude of deformation depth in $[cm]$;

A and B – crush coefficients set respectively in $[N/cm]$ и $[N/cm^2]$.

The main problems in the dynamic analysis of the obtained system of equations (1) and (4) can be classified in several groups:

1) Correct positions of vehicles on the plane of contact along the approach path prior to the moment of first impact.

2) Correct achievement of vector position of the velocity of the centre of mass before and after the impact.

3) The right choice of the tire-road friction coefficients along every stretch.

4) Correct choice of the value of the coefficient of restitution

5) The reading of the variable tire-road friction coefficient when the wheels are rotated around their own axles.

6) Adoption of speed survey approach by use of the Centre-of-Mass Motion Theorem (2).

5. Dynamic Analysis of Post Impact Motion of Vehicles

Undoubtedly, the proposed formula (2) is too general and does not cover the full dynamic analysis of the vehicle post-impact due to the fact that it does not count for the complexity of friction between tires and road surface, elasticity of suspension, damping and so on. Equation (1) clearly shows that not only the deformation energy of the two bodies, but also the post-impact vehicle velocity of the centre of mass and the angular speed of the vehicle are exhibited. If we apply the centre-of-mass motion theorem, it would be a rather inaccurate approach, for it would not be possible to estimate the kinetic energy for the rotation of the vehicle after the impact (Niehoff and Gabler, 2006; Jiang *et al.*, 2003).

A considerably more precise approach is to use a system of twelve differential equations that take into account friction forces, elasticity and suspension, damping forces, gravity force, air mass resistance, etc. (Daily *et al.*, 2006; Stucki, 1998; Hight *et al.*, 1985; Karapetkov and Uzunov, 2016).

The automobile is considered to be a multi-mass system (Fig. 2) and the initial conditions that meet the differential equations for vehicle motion determine the whole post-impact kinetic energy.

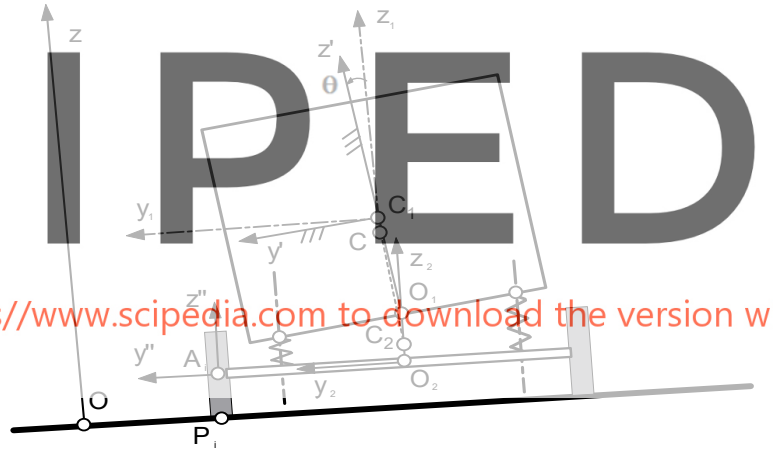

Figure 2. Rear view of the automobile

The analysis shows post-impact vehicle velocity of the centre of mass "u" and the angular velocity of the vehicle after the impact ω_z.

The differential equations of motion for each vehicle after impact, considered as a multi-mass spatial mechanical system, have the following views

$$m\ddot{x}_C = \sum_{i=1}^{4}[F_{ix}] + mg\sin\alpha - W_x\sqrt{\dot{x}_C^2 + \dot{y}_C^2}\dot{x}_C$$

$$m\ddot{y}_C = \sum_{i=1}^{4}[F_{iy}] + mg\sin\beta - W_y.\sqrt{\dot{x}_C^2 + \dot{y}_C^2}\dot{y}_C \qquad (14)$$

$$m\ddot{z}_C = \sum_{i=1}^{4}N_i - \frac{mg}{\sqrt{1 + tg^2\alpha + tg^2\beta}},$$

where: α – longitudinal slope of road; β – transverse slope of road.

According to the Work-Energy Theorem and its centre of mass in its relative motion on a translational moving reference frame starting with the centre of mass (briefly, relative motion to the centre of mass), we obtain

$$\frac{d\vec{K}_C^r}{dt} = \vec{M}_C^{(e)}, \tag{15}$$

where $\vec{M}_C^{(e)}$ is the moment of all external forces related to the centre of mass of the mechanic system.

According to König's theorem, the kinetic moment of the system is determined by the expression

$$\vec{K}_C^r = \vec{K}_C^{r1} + \vec{K}_C^{r2} + \vec{K}_C^{r3} = \left(\vec{K}_{C_1}^r + C\vec{C}_1 \times m_1\vec{V}_{C_1}^r\right) + \left(\vec{K}_{C_2}^r + C\vec{C}_2 \times m_2\vec{V}_{C_2}^r\right) + \\ +\left(\vec{K}_{C_3}^r + C\vec{C}_3 \times m_{kae}\vec{V}_{C_3}^r\right), \tag{16}$$

where $\vec{K}_C^r, \vec{K}_C^r, \vec{K}_C^r$ are kinetic moments respectively of the unsprung mass without flywheel kinetic energy storage system/FKESS/, sprung mass and flywheel kinetic energy storage system in relative motion to the centre of mass of the mechanical system; $\vec{K}_{C_1}^r, \vec{K}_{C_2}^r, \vec{K}_{C_3}^r$ - kinetic moments of respectively the unsprung and sprung mass in relative motion towards their centres of mass C_1, C_2 и C_3; m_1, m_2, m_{kae}- unsprung mass /without FKESS/, sprung mass and FKESS mass; $\vec{V}_{C_1}^r = \vec{V}_{C_1} - \vec{V}_C$, $\vec{V}_{C_2}^r = \vec{V}_{C_2} - \vec{V}_C$, $\vec{V}_{C_3}^r = \vec{V}_{C_3} - \vec{V}_C$ - relative velocity of the centres of mass respectively of the unsprung mass without FKESS, sprung mass and FKESS to translational moving reference frame starting at the centre of mass of the mechanical system.

The kinetic moment of the unsprung mass without the FKESS to its centre of mass in its relative motion around it in the projections of the coordinate axes permanently connected to the unsprung mass is of the kind

$$[K_{C_1}^r] = [J_{C_1}][\omega], \tag{17}$$

where: $[J_{C_1}]$ is a matrix of the mass inertia of the bodywork relative to the coordinate axes permanently connected to it

$$[J_{C_1}] = \begin{bmatrix} J_{x'} & -J_{x'y'} & -J_{x'z'} \\ -J_{x'y'} & J_{y'} & -J_{y'z'} \\ -J_{x'z'} & -J_{y'z'} & J_{z'} \end{bmatrix}, \tag{18}$$

while $[\omega]$ - matrix-column of the angular velocity projections on the same axes determined by Euler's formulas

$$[\omega] = \left[\omega_{x'} \;\; \omega_{y'} \;\; \omega_{z'}\right]^T = \begin{bmatrix} \sin\theta \sin\varphi \dot{\Psi} + \cos\varphi \dot{\theta} \\ \sin\theta \cos\varphi \dot{\Psi} - \sin\varphi \dot{\theta} \\ \cos\theta \dot{\Psi} + \dot{\varphi} \end{bmatrix}. \tag{19}$$

The kinetic moment of the sprung mass in its relative motion to its centre of mass C_2 is of the kind

$$\vec{K}_{C_2}^r = \sum_{i=1}^{4} \vec{K}_{kA_i}^r + \sum_{i=1}^{4} C_2\vec{A}_i \times m_{ki}\,\vec{V}_{kA_i}^r + \sum_{i=1}^{2} \vec{K}_{C_{mi}}^r + \sum_{i=1}^{2} C_2\vec{C}_{mi} \times m_{mi}\,\vec{V}_{C_{mi}}^r, \tag{20}$$

where: $\vec{K}_{kA_i}^r = J_{ky''i}\,\dot{\gamma}_i\,\vec{J}_{2i}'' + J_{kz''i}\left(\omega_2 + \dot{\vartheta}_{ki}\right)k_{2i}''$ is the kinetic moment of each of the wheels (resp. pair of wheels / to the centre of mass in relative motion around it with a mass of the wheel; $m_{ki,}$ – mass moment of inertia relative to its own axis of rotation; $J_{ky''i}$ mass moment of inertia relative to the radial axis; $J_{kz''i}$; $\vec{K}_{C_{mi}}^r = J_{mi}\,\omega_2\,\vec{k}_2$ – actual kinetic moment of each axle to its centre of mass in relative motion around it with a mass inertia moment related to the centre for the axle axis, which is parallel to the axis of z_2 / for trucks with dependent suspension; $\vec{V}_{kC_i}^r = \vec{V}_{kC_i} - \vec{V}_{C_2}$, $\vec{V}_{mC_i}^r = \vec{V}_{mC_i} - \vec{V}_{C_2}$, – corresponding relative velocities.

The kinetic moment of the FKESS to its centre of mass in relative motion around it in projections of central axes, parallel to the coordinate axes permanently connected to the unsprung mass, in matrix form is of the kind

$$\left[K_{C_3}^r\right] = \left[J_{C_3}\right][\omega_3], \tag{21}$$

where: $[\omega_3]$ is a matrix-column of the projections of the absolute angular velocity of FKESS $\vec{\omega}_3 = \vec{\omega} + \vec{\omega}_{kae}$ on central axes, parallel to the coordinate axes, permanently connected to the unsprung mass of the coordinate system $C_1x'y'z'$, determined by the Euler formula

$$[\omega_{kae}] = \left[\omega_{3x'} \;\; \omega_{3y'} \;\; \omega_{3z'}\right]^T = \begin{bmatrix}\omega_{x'} + \omega_{x'kae} \\ \omega_{y'} + \omega_{y'kae} \\ \omega_{z'} + \omega_{z'kae}\end{bmatrix} = \begin{bmatrix}\sin\theta \sin\varphi\, \dot{\Psi} + \cos\varphi\, \dot{\theta} + \omega_{kaex'} \\ \sin\theta \cos\varphi\, \dot{\Psi} - \sin\varphi\, \dot{\theta} + \omega_{kaey'} \\ \cos\theta\, \dot{\Psi} + \dot{\varphi} + \omega_{kaez'}\end{bmatrix}. \tag{22}$$

Here $\vec{\omega}_{kae}$ is actual angular velocity of the FKESS rotor.

The matrix $\left[J_{C_3}\right]$ has elements of mass inertia moments of FKESS related to its central axes, parallel to the coordinate axes, permanently connected to the unsprung mass

$$\left[J_{C_3}\right] = \begin{bmatrix} J_{3x'} & -J_{3x'y'} & -J_{3x'z'} \\ -J_{3x'y'} & J_{3y'} & -J_{3x'y'} \\ -J_{3x'z'} & -J_{3y'z'} & J_{3z'} \end{bmatrix}. \tag{23}$$

After replacing the above-mentioned quantities in (16), the theorem for the absolute derivative of the variable vector in a moving coordinate system is applied. For the unsprung mass, the moving coordinate system is permanently connected to the fixed coordinate system $C_1x'y'z'$, while for FKESS - a coordinate system starting with the rotor centre of mass and axes, parallel to the axes of the coordinate system, permanently connected to the unsprung mass coordinate system.

The following expression is obtained

$$\frac{d\vec{K}_{C_1}^r}{dt} + \vec{\omega} \times \vec{K}_{C_1}^r + \frac{d}{dt}\left[C\vec{C}_1 \times m_1\vec{V}_{C_1}^r\right] + \sum_{i=1}^{4}\frac{d}{dt}\left[J_{ky''i}\dot{\gamma}_i\vec{j}_{2i}'' + J_{kz''i}\left(\omega_2 + \dot{\vartheta}_{ki}\right)\vec{k}_{2i}''\right] + \\ + \sum_{i=1}^{4}\left[C_2\vec{A}_i \times m_{ki}\vec{V}_{kA_i}^r\right] + \sum_{i=1}^{2}\left[J_{m_1}\omega_2\vec{k}_2\right] + \sum_{i=1}^{2}\left[C_2\vec{C}_{mi} \times m_{mi}\vec{V}_{C_{mi}}^r\right] + \tag{24}$$

$$+ \frac{d}{dt}\left[C\vec{C}_2 \times m_2\vec{V}_{C_2}^r\right] + \frac{d\vec{K}_{C_3}^r}{dt} + \vec{\omega} \times \vec{K}_{C_3}^r + \frac{d}{dt}\left[C\vec{C}_3 \times m_3\vec{V}_{C_3}^r\right] = \vec{M}_{C_\omega}^{(e)},$$

where: $\vec{\omega}$ is angular velocity of the moving coordinate system, permanently connected to the unsprung mass.

After some transformations and projection of equation (24) on the axes permanently connected to the unsprung mass, the system of differential equations in matrix is obtained

$$\left\{\left[J_{C_1}\right] + \left[J_{C_3}\right]\right\}[\omega] = \left[M_{C_\omega}\right] + \left[M_{C_{3\omega}}\right] + \left[M_{C_a1}\right] + \left[M_{C_a2}\right] + \left[M_{C_a3}\right] + \left[M_{C_k}\right] + \left[M_{C_m}\right], \tag{25}$$

where: $[\dot{\omega}] = \left[\dot{\omega}_{x'} \;\; \dot{\omega}_{y'} \;\; \dot{\omega}_{z'}\right]^T$ is a matrix-column of the derivatives of the angular velocity projections on the coordinate axes permanently connected to the unsprung mass.

$$\left[M_{C_\omega}\right]\begin{bmatrix} M_{F_{x'}} + M_{N_{x'}} + J_{x'z'}\omega_{x'}\omega_{y'} - J_{x'y'}\omega_{x'}\omega_{z'} + \left(J_{y'} - J_{z'}\right)\omega_{y'}\omega_{z'} \\ +J_{y'z'}\left(\omega_{y'}^2 - \omega_{z'}^2\right) \\ M_{F_{y'}} + M_{N_{y'}} + J_{x'y'}\omega_{y'}\omega_{z'} - J_{y'z'}\omega_{x'}\omega_{y'} + \left(J_{z'} - J_{x'}\right)\omega_{x'}\omega_{z'} \\ +J_{x'z'}\left(\omega_{z'}^2 - \omega_{x'}^2\right) \\ M_{F_{z'}} + M_{N_{z'}} + J_{y'z'}\omega_{x'}\omega_{z'} - J_{x'z'}\omega_{y'}\omega_{z'} + \left(J_{x'} - J_{y'}\right)\omega_{x'}\omega_{y'} \\ +J_{x'y'}\left(\omega_{x'}^2 - \omega_{y'}^2\right) \end{bmatrix} \tag{26}$$

$$[M_{C_\omega}]\begin{bmatrix} J_{3x'z'}\omega_{3x'}\omega_{3y'} - J_{3x'y'}\omega_{3x'}\omega_{3z'} + (J_{3y'} - J_{3z'})\omega_{3y'}\omega_{3z'} + \\ +J_{3y'z'}\left(\omega_{3y'}^2 - \omega_{3z'}^2\right) \\ J_{3x'y'}\omega_{3y'}\omega_{3z'} - J_{3y'z'}\omega_{3x'}\omega_{3y'} + (J_{3z'} - J_{3x'})\omega_{3x'}\omega_{3z'} \\ +J_{3x'z'}(\omega_{3z'}^2 - \omega_{3x'}^2) \\ J_{3y'z'}\omega_{3x'}\omega_{3z'} - J_{3x'z'}\omega_{3y'}\omega_{3z'} + (J_{3x'} - J_{3y'})\omega_{3x'}\omega_{3y'} \\ +J_{3x'y'}\left(\omega_{3x'}^2 - \omega_{3y'}^2\right) \end{bmatrix}$$

$$M_{Ca1} = \begin{bmatrix} [(\vec{r}_C - \vec{r}_{C_1}) \times (\vec{a}_{C_1} - \vec{a}_C)]_{x'} \\ [(\vec{r}_C - \vec{r}_{C_1}) \times (\vec{a}_{C_1} - \vec{a}_C)]_{y'} \\ [(\vec{r}_C - \vec{r}_{C_1}) \times (\vec{a}_{C_1} - \vec{a}_C)]_{z'} \end{bmatrix}$$

$$M_{Ca2} = \begin{bmatrix} [(\vec{r}_C - \vec{r}_{C_2}) \times (\vec{a}_{C_2} - \vec{a}_C)]_{x'} \\ [(\vec{r}_C - \vec{r}_{C_2}) \times (\vec{a}_{C_2} - \vec{a}_C)]_{y'} \\ [(\vec{r}_C - \vec{r}_{C_2}) \times (\vec{a}_{C_2} - \vec{a}_C)]_{z'} \end{bmatrix}$$

$$M_{Ca3} = \begin{bmatrix} [(\vec{r}_C - \vec{r}_{C_3}) \times (\vec{a}_{C_3} - \vec{a}_C)]_{x'} \\ [(\vec{r}_C - \vec{r}_{C_3}) \times (\vec{a}_{C_3} - \vec{a}_C)]_{y'} \\ [(\vec{r}_C - \vec{r}_{C_3}) \times (\vec{a}_{C_3} - \vec{a}_C)]_{z'} \end{bmatrix}$$

$$[M_{Ck}] = -\begin{bmatrix} \left[\sum_{i=1}^{4} J_{ky''i}\,\ddot{\gamma}_i\,\vec{J}''_{2i} + \vec{\omega}_2 \times \sum_{i=1}^{4} J_{k2i}\,\ddot{\gamma}_i\,\vec{J}''_{2i} + \sum_{i=1}^{4}[J_{kz'i}(\dot{\omega}_2 + \ddot{\vartheta}_{ki}) + \right. \\ \left. +m_{ki}|C_2\vec{A}_i|^2\dot{\omega}_2]\vec{k}_2 \right]_{x'} \\ \left[\sum_{i=1}^{4} J_{ky''i}\,\ddot{\gamma}_i\,\vec{J}''_{2i} + \vec{\omega}_2 \times \sum_{i=1}^{4} J_{k2i}\,\ddot{\gamma}_i\,\vec{J}''_{2i} + \sum_{i=1}^{4}[J_{kz'i}(\dot{\omega}_2 + \ddot{\vartheta}_{ki}) + \right. \\ \left. +m_{ki}|C_2\vec{A}_i|^2\dot{\omega}_2]\vec{k}_2 \right]_{y'} \\ \left[\sum_{i=1}^{4} J_{ky''i}\,\ddot{\gamma}_i\,\vec{J}''_{2i} + \vec{\omega}_2 \times \sum_{i=1}^{4} J_{k2i}\,\ddot{\gamma}_i\,\vec{J}''_{2i} + \sum_{i=1}^{4}[J_{kz'i}(\dot{\omega}_2 + \ddot{\vartheta}_{ki}) + \right. \\ \left. +m_{ki}|C_2\vec{A}_i|^2\dot{\omega}_2]\vec{k}_2 \right]_{z'} \end{bmatrix}$$

$$[M_{Ck}] = -\begin{bmatrix} \sum_{i=1}^{2}\left[J_{mi} + m_{mi}|C_2\vec{C}_{mi}|^2\right]\dot{\omega}_2\vec{k}_{2x'} \\ \sum_{i=1}^{2}\left[J_{mi} + m_{mi}|C_2\vec{C}_{mi}|^2\right]\dot{\omega}_2\vec{k}_{2y'} \\ \sum_{i=1}^{2}\left[J_{mi} + m_{mi}|C_2\vec{C}_{mi}|^2\right]\dot{\omega}_2\vec{k}_{2z'} \end{bmatrix}$$

Here, m is the total mass of the vehicle; $m_{ki}\ /i = 1\div4/$ – mass of each of the wheels; $m_{mi}\ /i = 1\div2/$ – mass of each of the drives; $x_c,\ y_c, z_c$ – coordinates of the vehicle center of mass in relation to the fixed coordinate system; ψ, θ, φ – Euler angles of body's corners (unsprung mass); θ_k– average angle of rotation of the steering wheels around their axles; $\gamma_i\ /i = 1\div4/$ – angles of rotation of the wheels on their

own rotary axis; $\dot{\gamma}_i\ /i = 1 \div 4/$ – wheel angular velocity; $\vec{F}_i,\ /i = 1 \div 4/$ – friction forces in the wheels; $N_i\ /i = 1 \div 4/$ – normal reactions in the wheels; w – drag coefficient; $\vec{\omega}$ – angular velocity of the movable coordinate system $C_1x'y'z'$ permanently connected to the unsprung mass; $[\dot{\omega}] = \left[\dot{\omega}_{x'}\ \dot{\omega}_{y'}\ \dot{\omega}_{z'}\right]^T$ – matrix column of the derivatives of the projections of angular velocity on the permanently connected to the unsprung mass coordinate axes; $\vec{\omega}_2$ – angular velocity of the sprung mass and the constantly connected to it movable coordinate system $O_2x_2y_2z_2$; ω_{kae} – angular velocity of the flywheel (if available); $M_{F,N_{x'}}, M_{F,N_{y'}}, M_{F,N_{z'}}$ – moments of the frictional forces on the wheels and the normal reactions to the permanently connected to the vehicle coordinate axes; $\left[J_{C_1}\right]$ – matrix of the mass inertia of the bodywork related to the coordinate axes, permanently connected to it; $[\omega]$ – matrix column of the projections of angular velocity on the same axes determined by Euler's formula; $J_{ky''i}, J_{kz''i}\ /i = 1 \div 4/$ – mass inertia of each wheel relative to its own axis of rotation and its radial axis; J_{m_i} – $/i = 1 \div 2/$ – intrinsic mass moment of inertia of each of the drives relative to its central axis parallel to z_2; $\vec{F}_{i\tau}$ – tangential component of the friction force on the wheel; μ – coefficient of friction depending on the sliding speed of the contact spot, which is introduced graphically or analytically; r_i – radius of the wheel; f_i – coefficient of rolling friction; $[I_\gamma]$ – square matrix of coefficients in front of the actual angular accelerations of the drive wheels, depending on the wheel and engine inertia moments; $[\ddot{\gamma}]$ – matrix column of its own angular wheel accelerations, of which two or four are propulsive; M_{d_i}, M_{s_i} – corresponding engine and brake torque applied to each wheel

Coordinates of the centre of mass of the unsprung mass are defined by the expressions

$$\begin{aligned}
x_{C_1} &= x_C - \frac{m_3}{m_1+m_2+m_3}\left(a_{11}x'_{C_1} + a_{12}y'_{C_1} + a_{13}z'_{C_1}\right) - \\
&- \frac{m_2}{m_1+m_2+m_3}\left[a_{11}x'_{O_1} + a_{12}y'_{O_1} + a_{13}z'_{O_1} + \left(\cos\varphi_{z1}\,x_{2_{C2}} - \sin\varphi_{z1}\,y_{2_{C2}}\right)\right] \\
y_{C_1} &= y_C - \frac{m_3}{m_1+m_2+m_3}\left(a_{21}x'_{C_3} + a_{22}y'_{C_3} + a_{23}z'_{C_3}\right) - \\
&- \frac{m_2}{m_1+m_2+m_3}\left[a_{21}x'_{O_1} + a_{22}y'_{O_1} + a_{23}z'_{O_1} + \left(\sin\varphi_{z1}\,x_{2_{C2}} - \cos\varphi_{z1}\,y_{2_{C2}}\right)\right] \\
z_{C_1} &= \frac{m_2}{m_1+m_2+m_3}z_C - \frac{m_3}{m_1+m_3}\left(a_{31}x'_{C_3} + a_{32}y'_{C_3} + a_{33}z'_{C_3}\right) - \frac{m_2}{m_1+m_3}z_{C_2},
\end{aligned} \tag{27}$$

where: m_1 is the unsprung mass; m_2 – sprung mass; m_{kae} – mass of flywheel (if available); $a_{ij}\ /i = 1 \div 3;\ j = 1 \div 3/$ - elements of the matrix formed by the mentioned cosines between the axes of the permanently connected to the sprung mass coordinate system and the fixed coordinate system.

The angle of rotation of the coordinate system $O_2x_2y_2z_2$ relative to the fixed coordinate system is determined by the integral

$$\varphi_{z1} = \int_{\varphi_{z10}}^{\varphi_{z1}} \varphi_z dt = \int_{\varphi_{z10}}^{\varphi_{z1}} \left[\dot{\psi}(t) + \cos\vartheta(t)\,\dot{\varphi}(t)\right]dt. \tag{28}$$

Coordinates of the centre of mass of the sprung mass have the notation

$$\begin{aligned}
x_{C_2} &= x_{C_1} + a_{11}x'_{0_1} + a_{12}y'_{0_1} + a_{13}z'_{0_1} + \left(\cos\varphi_{z1}\,x_{2_{C2}} - \sin\varphi_{z1}\,y_{2_{C2}}\right), \\
y_{C_2} &= y_{C_1} + a_{21}x'_{0_1} + a_{22}y'_{0_1} + a_{33}z'_{0_1} + \left(\sin\varphi_{z1}\,x_{2_{C2}} - \cos\varphi_{z1}\,y_{2_{C2}}\right), \\
z_{C_2} &= const,
\end{aligned} \tag{29}$$

where:

m – total mass of the vehicle;

$\vec{a}_C$ – acceleration of the vehicle center of mass in relation to the fixed coordinate system;

$\vec{F}_i$ – forces acting on the vehicle, including friction, suspension elasticity, damping, air resistance.

The relative movement of the wheels, differential/s / and the engine is characterized by a system of four differential equations obtained by Lagrange method, which has the type

$$[I_\gamma][\ddot{\gamma}] = [M_\gamma], \quad M_{\gamma i} = \{F_{i\tau} r_i + sign\,(\dot{\gamma}_i)[M_{di} - f_i N_i - M_{si}]\}, \tag{30}$$

$\vec{F}_{i\tau}$ is tangential component of the tire-road friction force, the positive direction of which is taken backwards, in the more frequent cases of braking or loss of stiffness.

$$F_{i\tau} = \mu N_i \left[\frac{V_{Pix}}{V_{Pi}}\cos(\varphi_z) + \frac{V_{Piy}}{V_{Pi}}\sin(\varphi_z)\right], \tag{31}$$

where: $\mu(V_P)$ is friction coefficient depending on slipping speed on the contact spot; $\vec{r}_i$ – radius of the wheel; f_i – coefficient of rolling friction; $\vec{N}_i$ – normal reaction of the road on wheels; $[I_\gamma]$ – a square matrix of coefficients in front the actual angular acceleration of the drive wheels, depending on the moment of inertia of the wheels and the engine; $[\ddot{\gamma}]$ – a matrix-column of the actual angular acceleration of the wheels, two or four of which are propulsive.

6. Results

A front-impact car accident (Fig. 3) has been reconstructed and investigated with known total masses of vehicles and mass moment of inertia parameters (Vangi, 2009; Neptune *et al*., 1992; Campbell, 1974; Niehoff and Gabler, 2006; Stronge, 2000). Retrospective accident analysis was performed on damaged areas. Depth of vehicle deformations was recorded in six evenly distributed stretches (Fig. 4). The position of the two vehicles at the moment of impact was determined in relation to roadway with centroid and centre of mass position in a selected stationary coordinate system. The geometric position of the two cars after the impact is known according to the same coordinate system. Elasticity coefficient and suspension damping data were taken into account.

Initial computational process conditions for differential motion equations (14), (15) have the form of

$$\begin{aligned}
&x_{11} = 23.4\ m;\ y_{11} = 0.85\ m;\ \varphi_{11} = 8.0^o\\
&x_{21} = 27.2m;\ y_{21} = 0.82\ m;\ \varphi_{21} = 173.0^o\\
&x_{12} = 24.1\ m;\ y_{12} = 3.3\ m;\ \varphi_{12} = 54.5^o\\
&x_{22} = 26.8m;\ y_{22} = 2.0\ m;\ \varphi_{22} = 92.0^o\\
&u_{1x} = -0.2\ m/s;\ u_{1y} = 5.4\ m/s\\
&u_{2x} = -0.5\ m/s;\ u_{2y} = 2.9\ m/s\\
&u_1 = \sqrt{-0.2^2 + 5.4^2} = 5.4\ m/s = 19.4\ km/h;\ \omega_1 = -14.3\ s^{-1}\\
&u_2 = \sqrt{-0.5^2 + 2.9^2} = 2.9\ m/s = 10.4\ km/h;\ \omega_2 = -4.7\ s^{-1}.
\end{aligned} \tag{32}$$

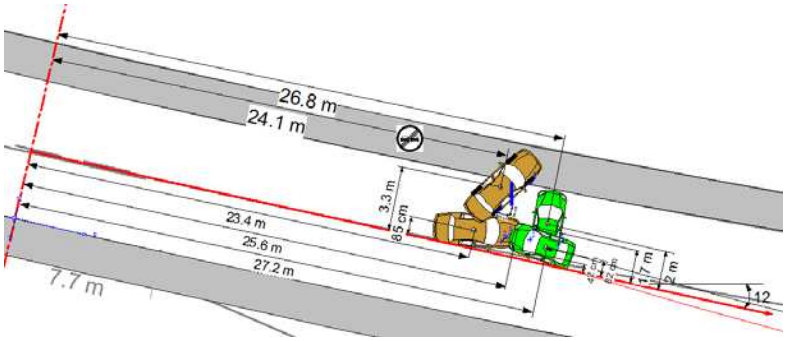

Figure 3. Impact process of front-impact car accident

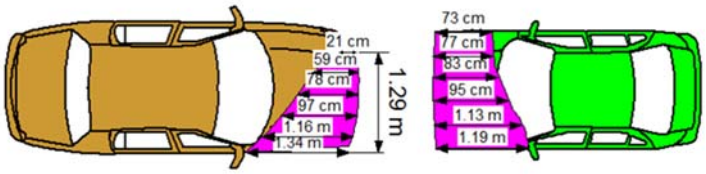

Figure 4. Car body deformations

Applying iterations. The initial conditions of the differential equations of motion are established and the solution to the problem of impact according to equations (1) and (5) results in the following data. presented in Table 1:

Table 1

PEUGEOT – 1; RENAULT – 2	Vehicle1	Vehicle 2
Total mass of the automobiles [kg]	1415.00 kg	980.00 kg
Mass moment of inertia J_{z1} and J_{z2} [kg m^2]	1850.00 kg m^2	750.00 kg m^2
Deformation depth at the first point of impact C1 in [cm]	134.00 cm	73.00 cm
Deformation depth at the second point of impact C2 in [cm]	116.00 cm	77.00 cm
Deformation depth at the third point of impact C3 in [cm]	97.00 cm	83.00 cm
Deformation depth at the fourth point of impact C4 in [cm]	78.00 cm	95.00 cm
Deformation depth at the fifth point of impact C5 in [cm]	59.00 cm	113.00 cm
Deformation depth at the sixth point of impact C6 in [cm]	21.00 cm	119.00 cm
Angle between the plane normal and the impact force in degrees [°]	10.00°	20.00°
Damage width in [m]	1.29 m	1.63 m
Angle between velocity direction and the center of mass before impact in degrees of X	8.00°	173.00°
Crash coefficient A in [N/cm]	362.00 N/cm	316.00 N/cm
Crash coefficient B in [N/cm^2]	48.30 N/cm^2	49.70 N/cm^2

After the numerical solution of the differential equations of motion using Matlab software tool, Simulink toolbox, the changes in the velocity projections of the centres of mass and the post-impact angular speeds for the vehicles in motion are obtained.

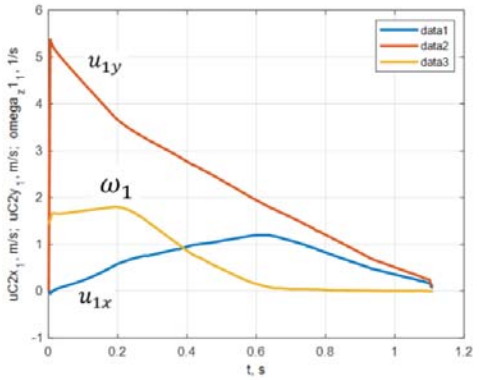

Figure 5. Changes in velocity projection of the centre of mass and in angular velocity of PEUGEOT after impact

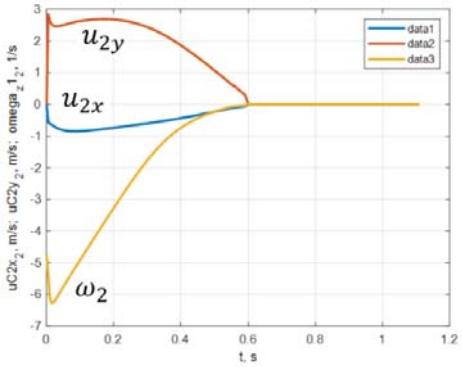

Figure 6. Changes in velocity projection of the centre of mass and in angular velocity of RENAULT after impact

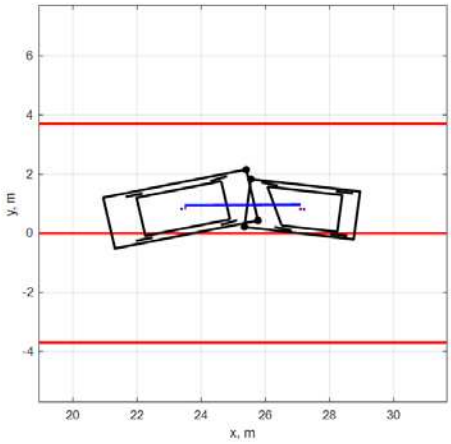

Figure 7. Position of the two vehicles at the moment of impact and direction of the impact impulse

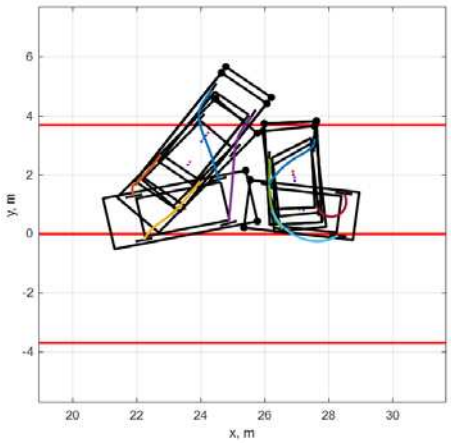

Figure 8. Computer simulation of vehicle motion after impact and direction of the impact impulse

After calculation (13), it is obtained
Deformation energy car PEUGEOT – 307523 Nm
Deformation energy car RENAULT – 462557 Nm
After solving equations (1) and (7) the following results are obtained:

$V_{1x} = 20.6\ m/s = 74.3\ km/h$ $V_{1y} = 3.5\ m/s = 12.5\ km/h$ $V_1 = 20.9\ m/s = 75.2\ km/h$

$V_{2x} = -31.7\ m/s = -114.4\ km/h$ $V_{2y} = 5.3\ m/s = 19.2\ km/h$ $V_2 = 32.1\ m/s = 112.0\ km/h$

$S_x = -28172\ Ns$ $S_y = 1752\ Ns$ $S = 28226\ Ns$

Test validity of the analysis can be done by applying the Impulse-Momentum Change Theorem for the two cars in the form of:

$$\vec{S} = m\vec{u} - m\vec{V}. \tag{33}$$

The following vector equation is obtained

$$\vec{V}_j = \vec{u}_j - \Delta\vec{V}_j, \quad j = 1.2. \tag{34}$$

A reconstruction model of vehicle impact speed for the centre of mass of both cars was built. The comparative analysis is shown in Figures 9 and 10.

Results are checked by the Impulse-Momentum Change Theorem (33). Verification includes parallelism of the two vectors dV_1 and dV_2.

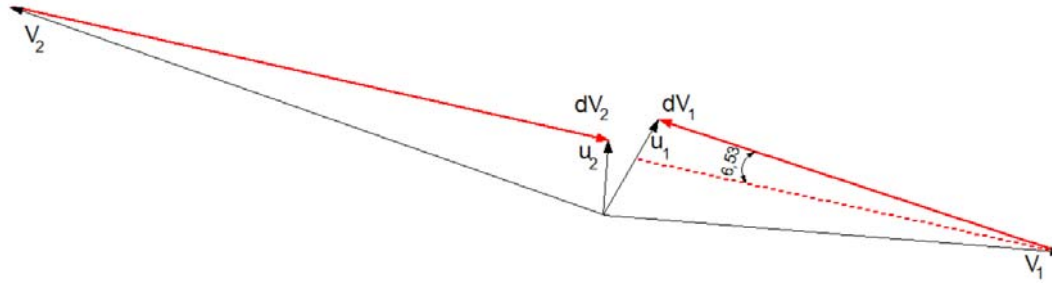

Figure 9. A reconstruction model of vehicle impact speed

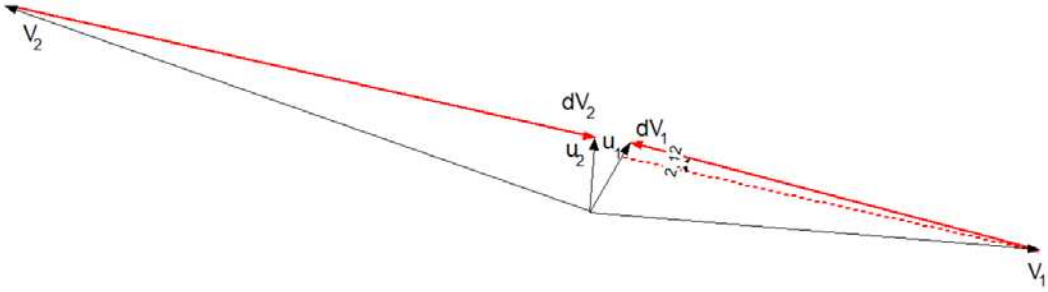

Figure 10. A reconstruction model of vehicle impact speed incorporating the principle of conservation of mechanical energy

In the first case (7), a vector analysis of the velocity change of the centre of mass related to impact was obtained without taking into account the angular velocity of the two vehicles after the impact. There is a difference in the parallelism of the two vectors of 6.53º.

In the second case, the results are more accurate, shown in the improved parallel of the two vectors obtained from the analysis of the post-impact velocity of the centres of mass of the two vehicles and including the angular rotation around their vertical axis, the improved coefficient reading of the tire-road friction, etc.

7. Conclusions

1. The dynamic analysis to determine linear and angular velocities of vehicle centre of mass includes a set of significantly more precise procedures that take into consideration the variability of the tire-road friction coefficient, the dynamic components of the suspension elasticity and damping.

2. A comparative analysis was carried out to solve the task of impact according to the proposed new approach and to the use of the attributed friction coefficient, as an indicator of the improved accuracy is the comparison of the parallelism of the vectors dV_1 and dV_2 based on the Impulse-Momentum Change Theorem (33). In the analysis, the accuracy of the study depends on the parallelism of the two vectors, where the divergence of 6.53° reached 2.12°.

3. The analysis shows that measurements of deformations of both vehicles regarding resultant deformation energy E_1 and E_2 should take into account maximum plastic deformation.

4. Vehicle impact testing methodology is the most accurate and applicable primarily to passenger cars. In cases of a truck crashes, mass moments of inertia should be well known. It is quite often that heavy trucks experience a significant change in the centre of mass as a result of load displacement, which in practice is hard to account for.

References

1. Campbell, K. (1974) Energy basis for collision severity, *SAE Technical Paper Series*, no. 740565.
2. Campbell, L. (1974) Energy Basis for Collision Severity. *SAE Paper* 740565.
3. Daily, J., Shigemura, N., Daily, J. (2006) Fundamentals of Traffic Crash Reconstruction. Jacksonville, Florida: Institute of Police Technology and Management, University of North Florida.
4. Hibbeler, R. (2004) *Engineering Mechanics: Dynamics. Upper Saddle River*, NJ: Prentice Hall, 10th ed.
5. Hight, P., Kent-Koop, D., Hight, R. (1985) Barrier equivalent velocity, delta v and CRASH3 stiffness in automobile collisions, *SAE Technical Paper Series*, no. 850437.

6. James, A., Neptune and James E. Flynn (1994) A Method for Determining Accident Specific Crush Stiffness Coefficients. *SAE Transactions.*
7. Jiang, T., Grzebieta, R. H., Rechnitzer, G., Richardson, S.; Zhao, X. L. (2003) Review of Car Frontal Stiffness Equations for Estimating Vehicle Impact Velocities. *The 18th International Technical Conference on the Enhanced Safety of Vehicles Conference (ESV*), Nagoya.
8. Karapetkov, S. (2005) Auto Technical Expertise, Technical University - Sofia, Bulgaria.
9. Karapetkov, S. (2010) *Investigation of road traffic accident, technical commentary on the lawyer*. Technical University of Sofia, Bulgaria.
10. Karapetkov, S., Uzunov, H. (2016) *Dynamics of transverse resistance of a car*. Didada Consult – Sofia, Bulgaria.
11. Mchenry, R., Mchenry, G. (1986) A Revised Damage Analysis Procedure for the CRASH Computer Program. *SAE Paper* 861894.
12. Neptune, J., Blair, G., Flynn, J. (1992) A method for quantifying vehicle crush stiffness coefficients, *SAE Technical Paper Series*, no. 920607.
13. Niehoff, P., Gabler, C. (2006) The Accuracy of WinSMASH Delta-V Estimates: The Influence of Vehicle Type, Stiffness, and Impact Mode." In: *the 50th Annual Proceedings of the Association for the Advancement of Automotive Medicine*, Annu Proc Assoc Adv Automot Med. 2006; 50: 73-89, Chicago, IL
14. Nolan, M., Preuss, A., Jones, L., O'Neill, B. (1998) An Update on Relationships between Computed Delta-Vs and Impact Speeds for Offset Crashes." In: *the Proceedings of the Sixteenth International Technical Conference on the Enhanced Safety of Vehicles* (Windsor, Canada, June 1998), Paper No. 98-S6-O-07.
15. Owsiański, R. (2007) Szacowanie energii deformacji nadwozi kompaktowych samochodów osobowych (Estimation of the bodywork deformation energy of compact passenger cars). Paragraf na Drodze No.4.
16. Prasad, K. (1990) CRASH3 Damage Algorithm Reformulation for Front and Rear Collisions. SAE 900098.
17. Schmidt, B., Haight, W., Szabo, T., Welcher, J. (1998) System-based energy and momentum analysis of collisions, In: *Accident Reconstruction: Technology and Animation VIII SP-1319,* no. 980026, Society of Automotive Engineers, Warrendale, PA, February.
18. Sharma, D., Stern, S., Brophy, J. (2007) An Overview of NHTSA's Crash Reconstruction Software WinSMASH. In: *Proceedings of the Twentieth International Conference on Enhanced Safety of Vehicles,* Paper No. 07-0211, Lyon, France.
19. Stronge, W. (2000) *Impact Mechanics*. Cambridge: Cambridge University Press.
20. Stucki, L., (1998) Fessahaie Comparison of Measured Velocity Change in Frontal Crash Tests to NASS Computed Velocity Change. *SAE 980649, Society of Automotive Engineers*.
21. Vangi, D. (2009) Simplified Method for Evaluating Energy Loss in Vehicle Collisions. *Accident Analysis and Prevention*, 41.
22. Wach, W. (2003) Analiza deformacji samochodu według standardu CRASH3. Część 2: Pomiar głębokości odkształcenia (Analysis of motor vehicle deformation according to the CRASH3 standard. Part 2: Measurement of deformation depth). Paragraf na Drodze No. 12.
23. Wicher, J. (2006) Energetyczne metody analizy, *Scientific and Educational Conference "Development of automotive engineering versus motor insurance",* Radom.